Development/Plasticity/Repair

Involvement of Bcl-2-Associated Transcription Factor 1 in the Differentiation of Early-Born Retinal Cells

Gaël Orieux,[1]* Laura Picault,[1]* Amélie Slembrouck,[1] Jérôme E. Roger,[1] Xavier Guillonneau,[1] José-Alain Sahel,[1,2] Simon Saule,[3] J. Peter McPherson,[4] and Olivier Goureau[1]

[1]Institut de la Vision, INSERM UMR_S968, CNRS UMR 7210, Sorbonne Universités, UPMC Univ Paris 06, 75012 Paris, France, [2]Centre Hospitalier National d'Ophtalmologie des Quinze-Vingts, INSERM-DHOS CIC 503, 75 571 PARIS Cedex 12, France, [3]CNRS-UMR 3347, INSERM U1021, Université Paris-sud11, Centre Universitaire, 91405 Orsay, France, and [4]Department of Pharmacology and Toxicology, University of Toronto, Toronto, Ontario M5S 1A8, Canada

Retinal progenitor proliferation and differentiation are tightly controlled by extrinsic cues and distinctive combinations of transcription factors leading to the generation of retinal cell type diversity. In this context, we have characterized Bcl-2-associated transcription factor (Bclaf1) during rodent retinogenesis. Bclaf1 expression is restricted to early-born cell types, such as ganglion, amacrine, and horizontal cells. Analysis of developing retinas in *Bclaf1*-deficient mice revealed a reduction in the numbers of retinal ganglion cells, amacrine cells and horizontal cells and an increase in the numbers of cone photoreceptor precursors. Silencing of *Bclaf1*expression by *in vitro* electroporation of shRNA in embryonic retina confirmed that Bclaf1 serves to promote amacrine and horizontal cell differentiation. Misexpression of Bclaf1 in late retinal progenitors was not sufficient to directly induce the generation of amacrine and horizontal cells. Domain deletion analysis indicated that the N-terminal domain of Bclaf1 containing an arginine-serine-rich and a bZip domain is required for its effects on retinal cell differentiation. In addition, analysis revealed that Bclaf1 function occurs independently of its interaction with endogenous Bcl-2-related proteins. Altogether, our data demonstrates that Bclaf1expression in postmitotic early-born cells facilitates the differentiation of early retinal precursors into retinal ganglion cells, amacrine cells, and horizontal cells rather than into cone photoreceptors.

Key words: **amacrine cells; Bclaf1; cone photoreceptors; horizontal cells; retina; retinal ganglion cells**

Introduction

The vertebrate retina is a laminar structure composed of seven cell types, all derived from a common pool of multipotent retinal progenitor cells (RPCs) (Livesey and Cepko, 2001; Cayouette et al., 2006; Bassett and Wallace, 2012). Retinogenesis follows an evolutionarily conserved, but overlapping, sequence with retinal ganglion cells (RGCs), amacrine cells (ACs), horizontal cells (HCs), and cone photoreceptors becoming postmitotic first, whereas rod photoreceptors, bipolar cells, and Müller glial cells are generated during a later wave of differentiation (Young, 1985; Rapaport et al., 2004). This sequence depends on both cell-extrinsic and cell-intrinsic factors (Livesey and Cepko, 2001; Cayouette et al., 2006; Bassett and Wallace, 2012) which determine both distinct and successive cell-fate choice by RPCs. Several converging lines of evidence point to specific transcription factors (homeoproteins, basic helix-loop-helix, forkhead/winged helix, basic motif-leucine zipper, etc.) as intrinsic retinogenic factors (Furukawa et al., 1997; Hatakeyama et al., 2001; Mears et al., 2001; Dyer et al., 2003; Li et al., 2004; Matter-Sadzinski et al., 2005; Fujitani et al., 2006; Jia et al., 2009; Swaroop et al., 2010). An increasing number of data indicates that post-transcriptional regulation at the mRNA level, such as alternative splicing regulation, RNA-binding proteins (Boy et al., 2004), and noncoding RNA processing (Decembrini et al., 2009; Georgi and Reh, 2010; Hwang et al., 2012; Maiorano and Hindges, 2012) also play a key role in retinal development.

Several transcriptomic analyses during rat retinal development, enabled us to identify a novel transcription factor in retinal development, namely Bcl-2-associated transcription factor 1 (Bclaf1; Roger et al., 2007). Although it was originally identified as a protein interacting with antiapoptotic members of the Bcl-2 family (Kasof et al., 1999), Bclaf1 actually does not share structural similarities with these proteins. The most prominent feature

Received July 29, 2013; revised Nov. 15, 2013; accepted Nov. 27, 2013.

Author contributions: G.O., L.P., J.-A.S., and O.G. designed research; G.O., L.P., A.S., and O.G. performed research; J.E.R., X.G., S.S., and J.P.M. contributed unpublished reagents/analytic tools; G.O., L.P., A.S., J.E.R., X.G., S.S., J.P.M., and O.G. analyzed data; G.O. and O.G. wrote the paper.

This work was financed by INSERM, UPMC-Université Paris 6 and Retina France association. This work was performed in the frame of the LABEX LIFESENSES (reference ANR-10-LABX-65) and was supported by French state funds managed by the Agence Nationale de la Recherche within the Investissements d'Avenir programme under reference ANR-11-IDEX-0004-02. The imaging facility was supported by "Departement de Paris" and by "Region Ile de France." L.P. was supported by the French Ministry of National Education Advanced Instruction and Research and by "Fédération des Aveugles de France." A.S. was supported by the Agence Nationale de la Recherche (GPiPS: ANR-2010-RFCS005). The work in the laboratory of J.P.M. was supported by the Canadian Lung Association/Ontario Thoracic Society and J.P.M. was the recipient of a Province of Ontario Early Researcher Award. We thank R. Hakem for mice, and Drs C. Craft and R. Molday for antibodies. We also thank S. Fouquet and D. Godefroy of the Institut de la Vision Imaging Facility, A. Ypsilanti for critical reading, and O. Anezofor and S. Thomasseau for technical assistance.

The authors declare no competing financial interests.

*G.O. and L.P. contributed equally to this work.

Correspondence should be addressed to Dr Olivier Goureau, Institut de la Vision, UMR S968, 17, Rue Moreau 75012 Paris, France. E-mail: olivier.goureau@inserm.fr.

J.E. Roger's present address: Neurobiology, Neurodegeneration and Repair Laboratory NIH, National Eye Institute, Bethesda, MD.

DOI:10.1523/JNEUROSCI.3227-13.2014

 0270-6474/14/341530-12$15.00/0

of the Bclaf1 sequence is the presence of an arginine-serine rich (RS) domain typically found in proteins involved in pre-mRNA splicing or mRNA processing and of two distinct domains, respectively homologous to the bZIP and to the Myb DNA-binding domains (Kasof et al., 1999; Haraguchi et al., 2004). In *vitro* studies have also implicated Bclaf1 in pathways that link transcriptional events to cell death, autophagy or DNA repair (Haraguchi et al., 2004; Liu et al., 2007; Rénert et al., 2009; Sarras et al., 2010; Lamy et al., 2013). However, several lines of evidence indicate that Bclaf1 has a much broader function and serves in various processes that are not typically related to Bcl-2 function (McPherson et al., 2009; Sarras et al., 2010). For instance, Bclaf1 participates in processes that regulate RNA metabolism (Merz et al., 2007; Bracken et al., 2008; Sarras et al., 2010) and studies conducted in *Bclaf1*-deficient mice revealed new functions of Bclaf1 in peripheral T-cell homeostasis and proper lung development (McPherson et al., 2009). In this study, we report a new function for Bclaf1 in retinal development during which Bclaf1 participates in regulating the differentiation of early-born retinal cells independently of interactions with Bcl-2-related proteins.

Materials and Methods

Animals. Timed pregnant C57BL/6J mice and Sprague-Dawley OFA were purchased from Charles River Laboratories. Bclaf1-deficient mice maintained in a C57BL/6J background have been described previously (McPherson et al., 2009). Embryos were obtained by mating *Bclaf1* heterozygote animals and were genotyped as previously described (McPherson et al., 2009). The day of vaginal plug corresponded to embryonic day (E)0, and the day of birth corresponded to postnatal day (P)0. Animals were killed according to the recommendations of our local ethical and animal care committee and eyes were dissected to recover neural retinal tissues (Authorization 75-865 delivered on April 30, 2010 by the Minister of Agriculture). The methods used to secure animal tissue complied with the Association for Research in Vision Ophthalmology Statement for the Use of Animals in Ophthalmic and Vision Research.

Retinal explants cultures and electroporation. Retina used for explants cultures were dissected in CO_2-independent medium (Life Technologies) and the central regions of the retinas were placed on polycarbonate filter discs (Dutscher). Cultures were maintained up to 7 d in DMEM/F12 medium with 10 mM HEPES, pH 7.0 containing 5% fetal calf serum and 100 μg/ml penicillin-streptomycin (Life Technologies), and half of medium was changed every 3 d.

For electroporation, the central regions of retinas from embryos (E16) and newborn (P0) pups were dissected and submerged in 1 mg/ml DNA as previously described (Roger et al., 2006). The retinas were oriented so that outer layer of the retina was facing the negative electrode. They were then subjected to five electric pulses at 30 V with 50 ms duration and 950 ms intervals using a CUY21 electroporator (CUY21 Single Cell BEX; Nepa Gene, Sonidel) using bath platinum plate electrodes on Petri dishes (CUY520P5, Nepa Gene). Explants were then placed on polycarbonate filter discs (Dutscher) and cultured as described above.

Cryosection and cell dissociation. For cryosectioning, retinal explants or dissected eyes were fixed for 30 min (explants) or 1–2 h (according to the developmental stage) in cold 4% paraformaldehyde (PFA) at 4°C and incubated in PBS, 30% sucrose (Sigma-Aldrich) 1 h (explants) or overnight (eyes) followed by an incubation at 37°C in PGS (PBS, 7.5% gelatin, Sigma-Aldrich; 10% sucrose) for 1 h. Eyes were embedded in PGS and frozen at −50°C in isopentane. Fourteen-micrometer-thick cryosections were collected. For cell dissociation, explants were detached from their filters and dissociated with trypsin as previously described (Roger et al., 2006). Dissociated cells were plated on glass slides coated with poly-D-lysine at 37°C for 2–3 h before fixation in cold 4% PFA for 10 min and immunostaining.

Immunostaining and image acquisition. Immunofluorescence staining of retinal sections or dissociated cells was performed as previously described (Roger et al., 2006). Briefly, slides were incubated for 1 h at room temperature with blocking solution (PBS containing 0.2% gelatin, and 0.1–0.5% Triton X-100) and then with the primary antibody overnight at 4°C. The following primary antibodies were used: mouse anti-AP2 (DSHB), mouse anti-Brn3a (Millipore), mouse and rabbit anti-Bclaf1 (BD Biosciences and Bethyl), rabbit anti-Calbindin (Swant), mouse anti-Calretinin (Millipore), rabbit anti-Cone arrestin (CAR; Millipore), mouse anti-CyclinD1 (Santa Cruz Biotechnology), mouse and rabbit anti-GFP (Roche and Clinisciences), mouse anti-glutamine synthetase (GS; Millipore), mouse anti-Lim1 (DSHB); rabbit anti-Otx2 (Millipore), rabbit anti-Pax6 (Millipore), rabbit anti-proliferating cell nuclear antigen (PCNA; Santa Cruz Biotechnology) rabbit anti-Protein Kinase Cα (PKCα, Santa Cruz Biotechnology), mouse anti-rhodopsin (R4D2, gift from Dr Molday, University of British Columbia, Vancouver, Canada), rabbit anti-recoverin (Millipore), rabbit anti-Retinoid acid receptor gamma (RXRγ; Santa Cruz Biotechnology), and rabbit anti-Sox9 (Millipore). Slides were washed three times in PBS with Tween 0.1% and then incubated for 1 h with appropriate secondary antibody conjugated with AlexaFluor 488 or 594 diluted at 1:500 in blocking buffer with 1:1000 diamidino-phenyl-indole (DAPI). TUNEL assays were performed using the *in situ* cell death detection kit (Roche Diagnostics) according to the manufacturer's recommendations. Fluorescent staining signals were captured with a DM6000 microscope (Leica Microsystems) equipped with a CCD CoolSNAPfx monochrome camera (Roper Scientific) or with an Olympus FV1000 confocal microscope equipped with 405, 488, and 559 nm lasers. Confocal images were acquired using a 0.52 μm step size and each image corresponds to the projection of 4–8 optical sections. MetaMorph software (Universal Imaging) was used to measure and analyze the intensity of fluorescent staining after cell dissociation of electroplated retinal explants. The same thresholds for fluorescent staining signals were used for a given antibody combination and experiment. For cell quantifications, retinal sections were scanned at high resolution (0.23 μm/pixel) with the Hamamatsu Nanozoomer Digital Pathology (NDP) 2.0 HT (fluorescence unit L11600-05) and the NanoZoomer's 3-CCD TDI camera (Hamamatsu Photonics). Quantifications were performed using the NDP viewer1.2.47 software with the NDPviewEx1.3.8 counter unit.

RT-PCR and quantitative-PCR. mRNA was prepared using a Nucleospin RNA II kit (Macherey Nagel) and cDNA synthesis was performed using the SuperScript II Reverse Transcriptase (Life Technologies), each according to the suppliers instructions. For cell sorting, a total of 10^5 cells GFP-positive dissociated cells were collected in lysis buffer (Nucleospin RNA II) using Vantage Sorter (BD Biosciences). PCR were performed in 25 μl final volume with TaqDNA polymerase (Life Technologies) and 10 μM of each forward and reverse primers (primers used for the identification of the isoforms of *Bclaf1:* a forward 5′-CCCGGCTAGCAGGAGAGGAGA-3′; b reverse 5′-CTATTCCTTTTCTTCTTTGCGT-3′; and c forward 5′-GAGGAACCTTTCGATGACAGAG-3′) according to the manufacturer's instructions. Cycling protocol was as follows: 95°C, 2 min; 32 cycles of 95°C, 30 s; 68°C, 30 s; and 72°C, 45 s, followed by a final extension step at 72°C for 5 min. PCR products were run on a 1.5% agarose gel stained with ethidium bromide and visualized under UV illumination.

For quantitative PCR, reactions were performed in a 20 μl final volume with Power SYBR Green PCR Master Mix (Life Technologies) and 0.25 μM primers (*Atoh7* forward 5′-ATGGCGCTCAGCTACATCATC-3′ and reverse 5′-CATAGGGCTCAGGGTCTACCT-3′; *Ascl1a* forward 5′-GCAACCGGGTCAAGTTGGT-3′ and reverse 5′-GTCGTTGGAGTAGTTGGGGG-3′; *Bclaf1* forward 5′-AAAGAGCCCTGAGATACACA-3′ and reverse 5′-CTTCTTTAAAAACTCTCTCGT-3′; *FoxN4* forward 5′-GAAAGCTTCAGCCTGGACAC-3′ and reverse 5′-TAGGCCGCATAGAGACCTGT-3′; *Ngn2* forward 5′-TCGGCTTTAACTGGAGTGCC-3′ and reverse 5′-GTGTGTTGTCGTTCTCGTGC-3′; *Ptf1a* forward 5′-CTACGGTCTCCCTCCTCTTG-3′ and reverse 5′-CCTCTGGGGTCCACACTTTA-3′; *Prox1* forward 5′-AGAAGGGTTGACATTGGAGTGA-3′ and reverse 5′-TGCGTGTTGCACCACAGAATA-3′; *S26* forward5′-AAGTTTGTCATTCGGAACATT-3′ and Reverse5′-GATCGATTCCTGACAACCTTG-3′) using the 7300 Real-Time PCR System (Life Technologies) according to the manufacturer's instructions. Gene expression threshold-cycle values were normalized to endogenous levels of S26. Samples

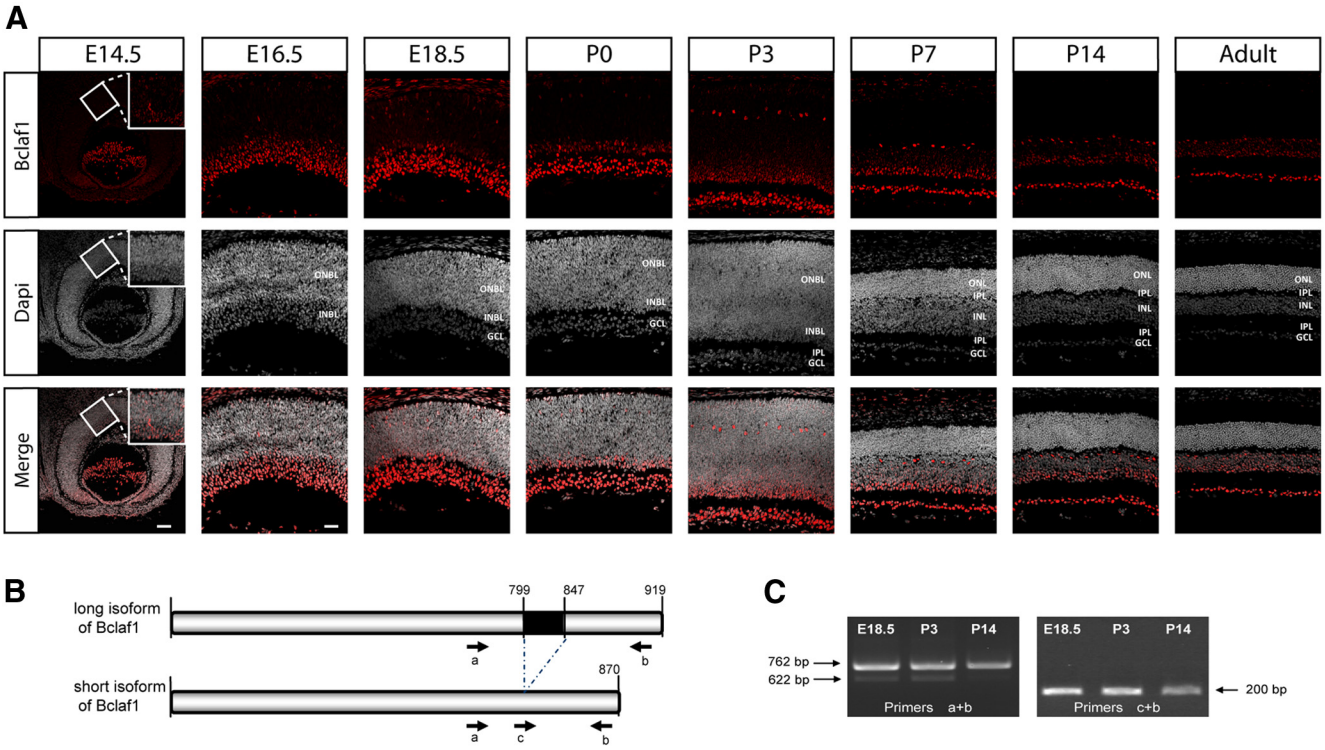

Figure 1. Characterization and expression pattern of Bclaf1 in the developing mouse retina. ***A***, Retinal sections from E14.5 to adulthood mice were stained with a rabbit-polyclonal antibody against Bclaf1. Bclaf1 expression is restricted to the INBL and the GCL from E14.5 to P3 and then to the INL until adulthood. Note that at P3 and later, a few Bclaf1+ cells are also found in the differentiating ONL and could potentially correspond to horizontal cells. The white boxed areas on E14.5 panels are twofold magnifications (top and right corner) to show the faintly labeled cells located in the center of the retina. Scale bars: 60 μm (E14.5), 30 μm (E16.5-adulthood). IPL, Inner plexiform layer; OPL, outer plexiform layer. ***B***, Schematic structure of short and long isoforms of Bclaf1. The black box corresponds to the deleted part in the short isoform of Bclaf1. The epitope recognized by the Bclaf1 polyclonal antibody maps to a region between residues 150 and 200, shared by the two isoforms. ***C***, Expression of the long and short isoforms of Bclaf1 in the retina at E18.5, P3, and P14 detected by PCR using specific primers able to amplify both isoforms (primers a + b) or only the short isoform (primers c + b).

were run in triplicate and corresponded to three independent biological samples.

Construction of shRNA vectors and pCIG overexpression vectors. The pU6-Bclaf1 small hairpin RNA (shRNA) was generated by ligation of the following annealed oligonucleotides into the pGSU6 RNAi vector (Genlantis) according to the supplier's instructions: 5′-GatccGCAGCTTC CGGCGACATTTgaagcttgAAATGTCGCCGGAAGCTGCtttttggaagc-3′ and 5′-ggccgcttccaaaaaaGCAGCTTCCGGCGACATTTcaagcttcAAATGTCG CCGGAAGCTGCg-3′. The GeneSilencer shRNA vector contain the U6 RNA polymerase III promoter, allowing optimal expression of shRNA and a GFP reporter gene under the control of CMV promoter. The ligation product was transformed into OneShot TOP10 chemically competent *Escherichia coli* cells (Life Technologies). Positive clones were identified by restriction enzymes analysis of purified plasmid and verified by DNA sequencing.

The rat *Bclaf1* (NM_001047852) was cloned using the gateway technology (Life Technologies) into a pCIG-eGFP vector that contained an internal ribosome entry site sequence to generate enhanced green fluorescent protein (eGFP) under the control of the same β-actin promoter (Roger et al., 2006). Specific primers with incorporated attB sites (available on request) were designed to amplify full-length of the *Bclaf1*, *Bclaf1*-DC210, and *Bclaf1*-DN384. The PCR reactions were performed with Platinium TaqDNA Polymerase High Fidelity (Life Technologies) using mice genomic DNA (or pCIG-Bclaf1-eGFP for mutant construction) as the template. The different specific PCR products purified after gel agarose electrophoresis were then subcloned into the entry clone (pDONR221 vector) by BP Clonase Reaction (Life Technologies). OneShot TOP10 chemically competent E.coli cells were transformed by using 5 μl of the BP reaction. Positive clones were identified by restriction enzyme analysis of purified plasmid and verified by DNA sequencing. Each pDONR221-Bclaf1 construct was recombined in the presence of LR recombinase (Life Technologies) into a pCIG-eGFP gateway. OneShot TOP10 chemically competent *E. coli* cells were transformed and positive clones were identified by restriction enzyme analysis.

Western blot analysis. Protein extracts were collected in lysis buffer (20 mM NaH_2PO_4, 250 mM NaCl, 30 mM NaPPi, 0.1% NP40, 5 mM EDTA, 5 mM DTT) containing protease inhibitors from transfected DF1 fibroblast cells. Homogenates were sonicated and centrifuged for 5 min at 5000 g, and then 20 μg of the supernatant were subjected to SDS-PAGE, as previously described (Roger et al., 2006). Antibody binding was revealed by the Enhanced Chemiluminescence System Plus (GE Healthcare) on X-Ray film.

CAT assay. Baby hamster kidney (BHK)-21 cells, cultured as previously described (Planque et al., 2001), were seeded 24 h before transfection with polyethylenimine, Exgen 5000 (Euromedex) reagent according to the instructions of the manufacturer. Expression plasmids (900 ng) were cotransfected and the total amount of transfected DNA was kept constant by addition of empty expression vector. A pcDNA3-LacZ was cotransfected for normalization of CAT assays by controlling the galactosidase activity. CAT assays were performed as described previously (Planque et al., 2001). Levels of CAT activity were quantified after exposure of the thin layer chromatograms to a PhosphorImager screen (GE Healthcare).

Quantitative analysis. In the *Bclaf1*$^{-/-}$ and wild-type (WT) mice, the number of cells expressing the different markers was quantified by averaging the total number of positive cells on three different retinal sections centered on the optic nerve. We examined retinas from at least three *Bclaf1*$^{-/-}$ and control littermate mice. For quantification of dissociated cells that were immunolabeled as a monolayer, a minimum of 300 and up to 1000 cells per sample were counted using MetaMorph software (Universal Imaging). Quantification of marker staining is expressed as mean ± SEM. Statistical analysis was performed using Prism 6 (Graph-

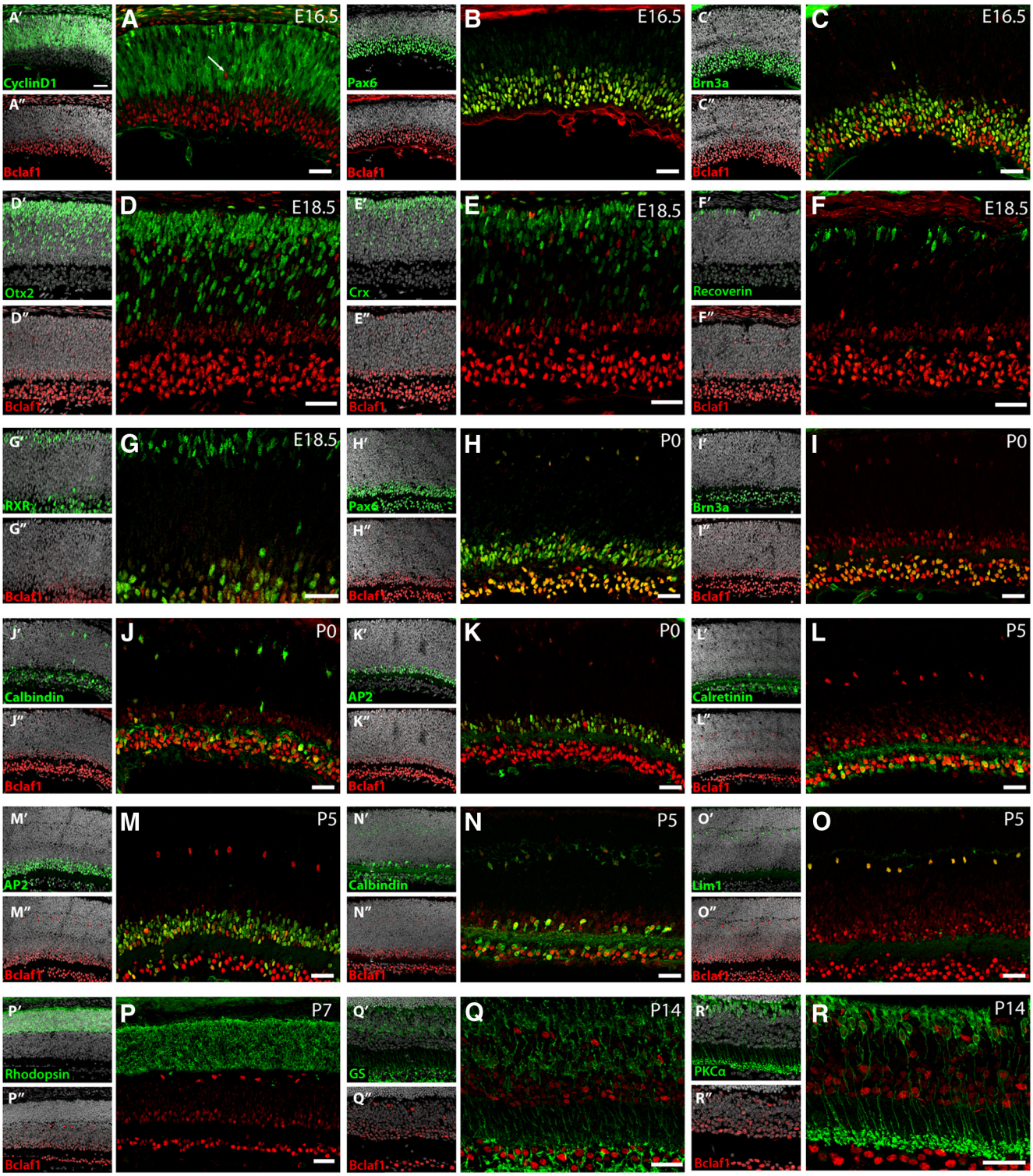

Figure 2. Expression of Bclaf1 in early-born retinal cells except cone photoreceptors. Sections of central retina close to the optic nerve at E16.5 (***A–C***), E18.5 (***D–G***), P0 (***H–K***), P5 (***L–O***), P7 (***P***), and P14 (***Q***, ***R***) were immunostained for Bclaf1 (red) and various cell-type markers (green). Small panels display the distribution of labeled cells for each specific marker in the retina visualized by DAPI counterstaining (gray). Large panels (merge) show that Bclaf1 is not expressed in postmitotic CyclinD1+ cells (***A***); note that the Bclaf1+ cell (arrow) visible in the ONBL (***A***) is cyclinD1-negative unlike virtually all other cells in this layer. At E16.5, nearly all Bclaf1+ cells express Pax6 (***B***) and all Brn3a+ RGCs express Bclaf1 (***C***). Conversely, in the ONBL, markers of precursors (Otx2, Crx,) or differentiating (recoverin) photoreceptors do not colocalized at E18.5 with Bclaf1 (***D–F***). Similarly, RXRγ+ cells located in the upper surface of the ONBL (E18.5), corresponding to cone-photoreceptor precursors, do not express Bclaf1 (***G***). At P0 and P5, markers of RGCs (Brn3a, ***I***) or amacrine cells, such as AP2 (***K***, ***M***), Pax6 (***H***), calretinin (***L***), and calbindin (***J***) colocalize with Bclaf1. Horizontal cells, identified at P5 by calbindin (***N***) or by Lim1 (***O***) are Bclaf1+. At P7 or P14, late born cells, i.e., rod-photoreceptors (rhodopsin+, ***P***) Müller glial cells (GS+, ***Q***) and bipolar cells (PKCα+, ***R***) do not express Bclaf1. Scale bars, 30 μm.

Pad) with Mann–Whitney test for all pair wise analysis. Values of $p < 0.05$ were considered statistically significant.

Results

Bclaf1 is expressed in differentiating early-born Pax6-positive neurons in the retina

Spatiotemporal analysis of Bclaf1 expression by immunostaining revealed that Bclaf1 is present in the retina from E14.5 to adulthood (Fig. 1). A clear expression was detected in the inner neuroblastic layer (INBL) at E16.5 (Fig. 1*A*) and also in the ganglion cell layer (GCL) at E18.5. From E18.5 to P3, Bclaf1 was expressed in the GCL and in the INBL that corresponds mainly to the differentiating inner nuclear layer (INL). At P3, a few sparsely labeled cells were also found in the differentiating outer nuclear layer (ONL; Fig. 1*A*). At P7, Bclaf1 remained expressed in the GCL and INL and its expression was restricted to these two nuclear layers in adulthood (Fig. 1*A*). Because both a short and long isoform of Bclaf1 have been described in human and mice tissue RT-PCR experiments were performed on mRNA extracts from mice retinas at several stages of development with primers specifically designed to discriminate the different Bclaf1 isoforms (Fig. 1*B*). A set of primer (a and b) hybridizing on both sides of the region lacking in the short isoform (Fig. 1*B*) allowed the amplification of two fragments corresponding to the short and the long isoforms at E18.5, P3, and P14. (Fig. 1*C*). The expression of the Bclaf1 short isoform was confirmed by defining a forward primer (c) that hybridized only with the cDNA sequence of this isoform (Fig. 1*B*,*C*).

To identify the retinal cell types that express Bclaf1, a series of double immunostaining experiments were performed on retinal sections at different stages of development. During embryonic stages, Bclaf1 expression was restricted to postmitotic precursors that are both cyclinD1-negative (Fig. 2*A*) and Pax6-positive (Fig. 2*B*), including Brn3a-positive differentiating RGCs (Fig. 2*C*). Conversely, Bclaf1 was not expressed by RXRγ-positive cells located in the upper part of the retina and corresponding to cone photoreceptor precursors (Fig. 2*G*) and did not colocalize with markers of photoreceptor precursors, such as Otx2, Crx, and recoverin (Fig. 2*D–F*). From P0 to P5, Bclaf1 was still expressed by early-born retinal cells in the differentiating inner retina as identified by immunostaining for Pax6 (ACs, HCs, and RGCs; Fig. 2*H*), Brn3a (RGCs; Fig. 2*I*), calbindin (ACs and HCs; Fig. 2*J*,*N*), AP2 (ACs; Fig. 2*K*,*M*), calretinin (ACs; Fig. 2*L*), or Lim1 (HCs; Fig. 2*O*). At later postnatal stages, P7 and P14, Bclaf1 expression was found in RGCs, ACs, and HCs but not in rod photoreceptors (rhodopsin-positives), Müller glial cells (GS-positives), and bipolar cells (PKCα-positives; Fig. 2*P–R*). In the adult retina, the pattern of Bclaf1 expression remained unchanged compared with its expression profile observed in immature postnatal retina (Fig. 3). Bclaf1 colocalized with markers of RGCs (Pax6, Brn3a), ACs and/or HCs (Calretinin, Calbindin and Lim1) and did not colocalized with markers of Müller glial cells (Sox9), rod photoreceptors (rhodopsin), and bipolar cells (PKCα). Altogether, these findings indicate that Bclaf1 was expressed in early-born retinal cells with the exception of the cone photoreceptors.

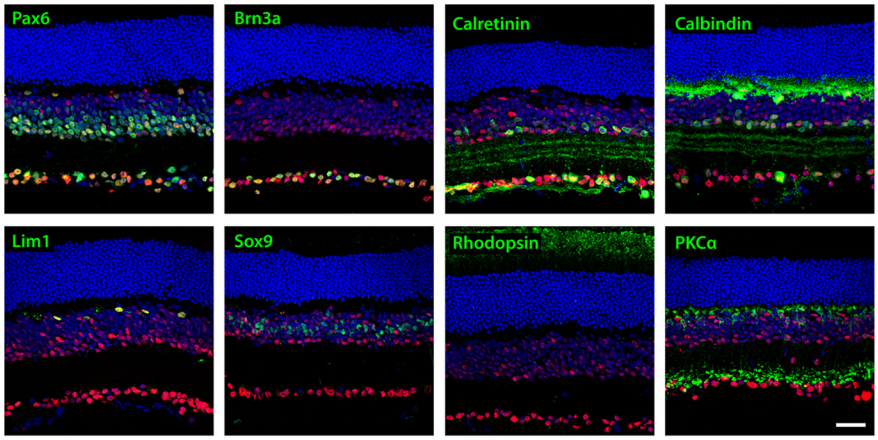

Figure 3. Expression of Bclaf1 in the adult retina. Retinal sections from adult mice were visualized by DAPI counterstaining (blue) and double-stained for Bclaf1 (red) and for the indicated marker (green). Confocal microscopic acquisitions show that Bclaf1 is expressed in Pax6+ cells, corresponding to RGCs (Brn3a), ACs (calretinin, calbindin), and HCs (Lim1, calbindin). Bclaf1 never colocalized with Rhodopsin, a rod-photoreceptor marker, PKCα, a bipolar cell marker, or Sox9, a marker of Müller glial cells. Scale bar, 30 μm.

Delay and defect of early-born retinal cell differentiation in absence of Bclaf1

To understand the function of Bclaf1, we analyzed the retinal phenotype of *Bclaf1*-deficient (*Bclaf1*$^{-/-}$) mice (McPherson et al., 2009). At E14.5, when Pax6 is expressed throughout the retina, the density of Pax6-positive cells showed no differences between *Bclaf1*$^{-/-}$ and WT retinas (data not shown). However, at E16.5 and E18.5, when Pax6 expression is progressively restricted to postmitotic cells, we observed a reduction in the density of Pax6-positive cells in *Bclaf1*-deficient retina compared with WT retina (Fig. 4). Consistent with the absence of expression of Bclaf1 in mitotic retinal progenitor cells, we did not observe any difference in the density of both CyclinD1- and PCNA-positive cells between WT and Bclaf1$^{-/-}$ retina (Fig. 4*A*,*B*). Regarding late-born cells, no differences were observed at E18.5 in the density of Otx2-positive precursors or differentiating photoreceptors (Crx- or recoverin-positives) between *Bclaf1*$^{-/-}$ and WT retina (Fig. 4). Because Pax6 is expressed in differentiating RGCs, ACs, and HCs, quantitative analysis of these three populations was performed using specific markers (Fig. 5*A–F*). At E14.5, the density of Brn3a-positive RGCs was reduced by 55.9% in *Bclaf1*-deficient retina compared with WT retina (Fig. 5*D*). At E16.5, the density of Brn3a-positive cells was still decreased in *Bclaf1*$^{-/-}$ retina (minus 35.5%; Fig. 5*A*,*D*), whereas at E18.5 the difference between *Bclaf1*$^{-/-}$ and WT retina was reduced to 14.4%, a statistically nonsignificant difference (Fig. 5*D*). The density of ACs/HCs immunoreactive for Calbindin was not significantly modified at E16.5 (Fig. 5*E*), but was significantly reduced in *Bclaf1*$^{-/-}$ retina at E18.5 (Fig. 5*B*,*E*). Indeed, the density of calbindin-positive ACs (GCL/INBL) and calbindin-positive HCs [outer neuroblastic layer (ONBL)] was lower in E18.5 *Bclaf1*$^{-/-}$ retina compared with WT: 88.5 ± 10.4 cells/mm versus 119.5 ± 10.7 cells/mm for ACs ($n = 3$; $p < 0.05$) and 31.1 ± 2.6 cells/mm versus 49.5 ± 3.4 cells/mm for HCs ($n = 3$; $p < 0.05$). Evaluation of apoptosis by TUNEL experiments in *Bclaf1*$^{-/-}$ and WT showed the presence of rare positive cells at E14.5, E16.5, and E18.5 retinas with no difference between both genotypes (data not shown). This suggests that the reduced number of early-born cell types observed in *Bclaf1*$^{-/-}$ retinas is not caused by an increase in cell death. Interestingly, RXRγ immunostaining at E18.5 (Fig. 5*C*,*F*) demonstrated that the density of cone photoreceptors, that do not

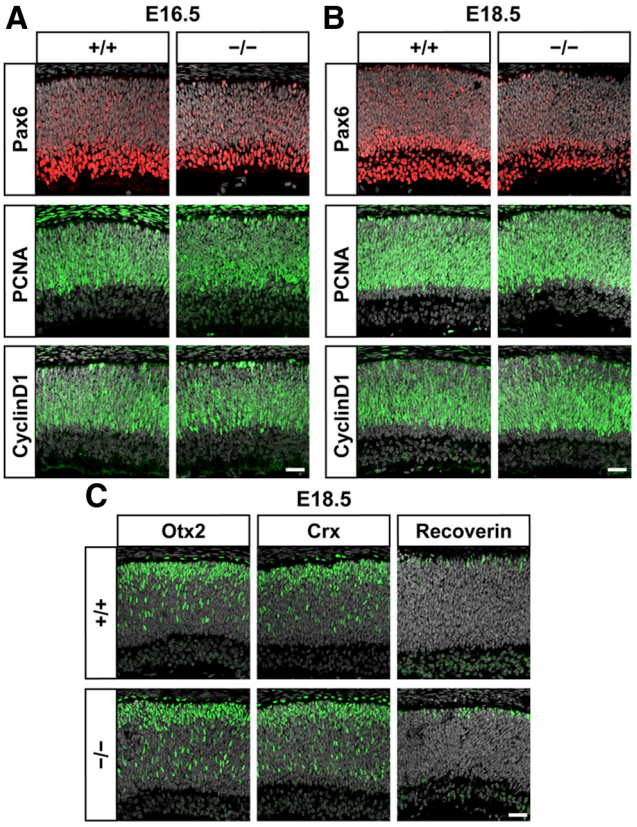

Figure 4. Early but not late lineage is affected in Bclaf1-deficient mice embryos. Immunostaining for Pax6 (red), cyclinD1, PCNA, Otx2, Crx, or recoverin (green) on retinal sections from WT and Bclaf1-deficient mice at E16.5 (***A***) or E18.5 (***B***, ***C***). Sections were counterstained with DAPI (gray). The density of Pax6+ cells, corresponding to early-born cell populations, is reduced in absence of Bclaf1 at E16.5 and E18.5. At the same stages, no difference is observed in the density of mitotic cells (progenitors) identified with CyclinD1 or PCNA between *Bclaf1* $^{-/-}$ and WT retina. The density of precursors of late born retinal cells (identified with Otx2, Crx, or recoverin) is not modified at E18.5 in *Bclaf1* $^{-/-}$ retina. Scale bar, 30 μm.

express Bclaf1, was increased by twofold in *Bclaf1* $^{-/-}$ retina (192 ± 25.2 cells/mm) compared with WT retina (99 ± 6.6 cells/mm, $n = 3$, $p < 0.05$).

As we observed that the impairment in RGC generation was resolved at E18.5 in *Bclaf1* $^{-/-}$ retinas *in situ*, we questioned whether the defect observed in AC and HC generation at E18.5 in *Bclaf1* $^{-/-}$ retinas could also be compensated at later stages. *Bclaf1*-deficient mice present a considerable perinatal mortality (McPherson et al., 2009). Accordingly we shifted to an *ex vivo* approach using retinal explant cultures (Roger et al., 2006; Lelièvre et al., 2012). Retinas were explanted at E18.5 and analyzed by immunohistochemistry after 7 d *in vitro* (DIV). At this stage, the density of HCs (Lim1-positives) was 17.0% lower in *Bclaf1* $^{-/-}$ retinal explants compared with WT explants (Fig. 5*G*,*H*). ACs (calretinin-positives) were also less numerous in *Bclaf1* $^{-/-}$ retinal explants with a decrease in density of 31.4% (Fig. 5*G*,*H*). The density of Calbindin-positive cells, including both HCs and a subpopulation of ACs, was reduced by 17.6% in *Bclaf1* $^{-/-}$ compared with WT retinas (Fig. 5*G*,*H*). At the same stage (E18.5 + 7 DIV), immunostaining for arrestin revealed that the number of positive cells is increased by 35% in Bclaf1 $^{-/-}$ retinal explants compared with WT explants (Fig. 5*G*,*H*), confirming the increase of cone-photoreceptors density previously observed with RXRγ labeling at E18.5 (Fig. 5*C*,*F*). The substantial cell death of RGCs found in retinal explants prevented us from analyzing this population.

Because we initially identified Bclaf1 from transcriptomic analyses during rat retinal development (Roger et al., 2007), we next investigated whether the functional invalidation of *Bclaf1* in rat embryonic retina could reproduce the retinal phenotype observed in *Bclaf1* $^{-/-}$ mice. We first confirmed that the expression profile of Bclaf1 in the rat retina was indeed identical to that observed in the mouse retina (Fig. 6*A*). Retinal explants from E16 rat embryos were electroporated with a pU6-shBclaf1-eGFP or a control pU6-shLuciferase-eGFP vector. Five DIV after electroporation, a significant decrease in Pax6-positive cells among the GFP-positive population was observed in shBclaf1-electroporated explants (35.2 ± 1.4%) compared with shLuciferase-electroporated control explants (47 ± 3.6%; $n = 3$, $p < 0.05$; Fig. 6*B*,*C*). Bclaf1 silencing decreased the number of GFP-positive ACs immunoreactive for AP2 or calretinin by 29.4 and 23.0%, respectively (Fig. 6*B*,*D*) and the density of GFP-positive HCs immunoreactive for Lim1 by 24.3% (Fig. 6*B*,*E*). Calbindin immunostaining confirmed the reduction of both AC and HC number, whereas 6.1 + 0.99% calbindin-positive cells was present in control only and 1.82 + 0.48% remained after Bclaf1 silencing (Fig. 6*B*). No significant difference in the number of apoptotic cells (TUNEL-positive) was observed between shBclaf1-electroporated explants and control explants (Fig. 6*B*), precluding the fact that cell death causes the decrease in different cell type numbers upon silencing of Bclaf1. These results were consistent with the data we observed in the *Bclaf1* $^{-/-}$ mice and strongly confirmed a role for Bclaf1 in the differentiation of Pax6-positive early-born retinal cells.

Overexpression of Bclaf1 in late RPCs hinders the differentiation of rod photoreceptors but fails to promote early-born retinal cell fate

We next examined whether Bclaf1 overexpression in late RPCs, that do not normally express this factor, could modify their cell fate and promote their differentiation into neurons with an "early-born" phenotype. The effective expression of Bclaf1 cloned into a pCIG-eGFP (Roger et al., 2006) vector has been verified at the protein level by Western blotting in DF1 cells (see Fig. 8*B*). After 7 DIV, overexpression of Bclaf1 led to 45.4% increase in the Pax6-positive fraction in dissociated cells from P0-electroporated explants (Fig. 7*A*). However, quantification of the proportion of ACs and HCs identified with calretinin and calbindin revealed no significant changes following Bclaf1 overexpression (Fig. 7*A*). As Bclaf1 seems unable to promote AC and HC differentiation, we next sought to determine the effect of forced Bclaf1 expression in the regulation of genes required for early-born AC and HC specification. q-PCR performed on mRNA extracts from FACS-isolated GFP-positive cells 36 h after electroporation revealed no changes in the mRNA expression of three transcription factors required for AC or HC specification (Dyer et al., 2003; Li et al., 2004; Fujitani et al., 2006), notably *Ptf1a*, *FoxN4*, and *Prox1* despite a sixfold increase in *Bclaf1* expression (Fig. 7*B*). This indicates that Bclaf1 does not act as a positive transcriptional regulator of genes required for AC/HC specification. Moreover, we also observed a significant decrease in the fraction of rhodopsin-positive photoreceptors in Bclaf1-electroporated explants (22.2 ± 1.9%) compared with controls (50.1 ± 1.9%; $n = 3$; $p < 0.01$; Fig. 7*C*). To test the possibility that forced Bclaf1 expression might induce rod apoptosis, TUNEL staining was performed. Despite a low number of positive cells, we observed a threefold increase in the number of TUNEL-positive cells among the GFP-positive population in the ONL of explants overexpressing Bclaf1 as compared with control ex-

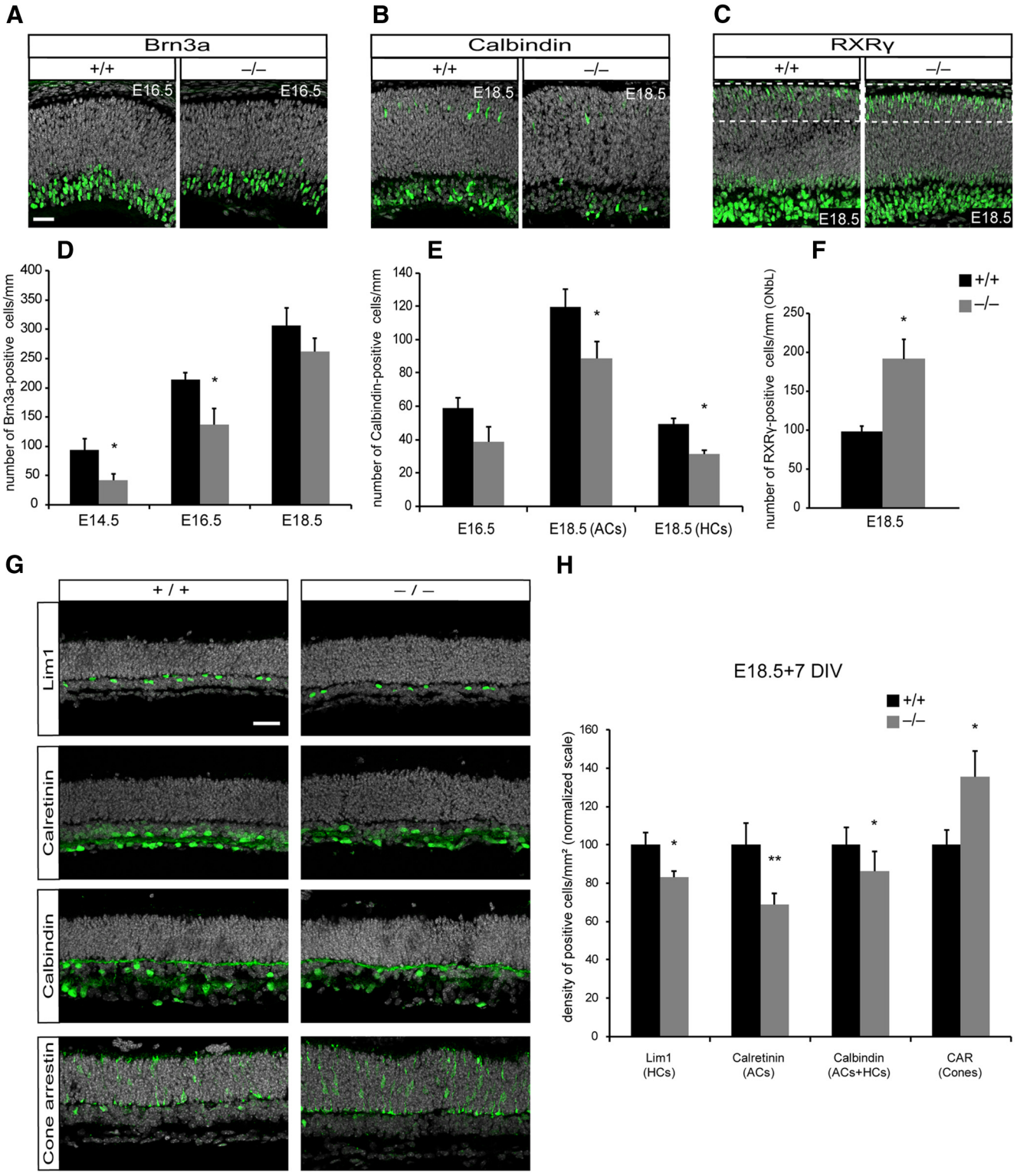

Figure 5. Bclaf1-deficient retinas display defects in the development of early-born cells. ***A–F***, Retinal sections from E14.5 to E18.5 *Bclaf1* $^{-/-}$ mice or WT littermate were stained for Brn3a (***A***), calbindin (***B***), or RXRγ (***C***). The density (number of cells per mm) of Brn3a+ RGCs is lower in *Bclaf1* $^{-/-}$ compared with WT retina at E14.5 (minus 55.9%), E16.5 (minus 35.5%), but not at E18.5 (***D***). The density of calbindin+ ACs in the innermost part of the INBL and calbindin+ HCs located in the ONBL is reduced at E18.5 in *Bclaf1* $^{-/-}$ retina (minus 26% and 36.7%, respectively) (***E***). The density of cone-photoreceptor precursors (RXRγ+ cells) is increased by 93% in *Bclaf1* $^{-/-}$ compared with WT retina at E18.5 (***F***). RXRγ+ cells were quantified in the ONBL only (dotted line delimited area) to exclude nonphotoreceptor RXRγ+ cells. ***G***, Sections from retinal explants (E18.5 + 7 DIV) of *Bclaf1* $^{-/-}$ mice or WT littermate were stained for Lim1, calretinin, calbindin, or cone arrestin (green) and counterstained for DAPI (gray). ***H***, The density of Lim1+ (HCs), calretinin+ (ACs), and calbindin+ cells (HCs and ACs) at E18.5 + 7 DIV was reduced in *Bclaf1* $^{-/-}$ retinal explants compared with WT, whereas the density of CAR+ cells (cone photoreceptors) was higher. Error bars indicate SEM and an asterisk a significant statistical difference (*$p < 0.05$, **$p < 0.01$; $n = 4–5$). Scale bars, 30 μm.

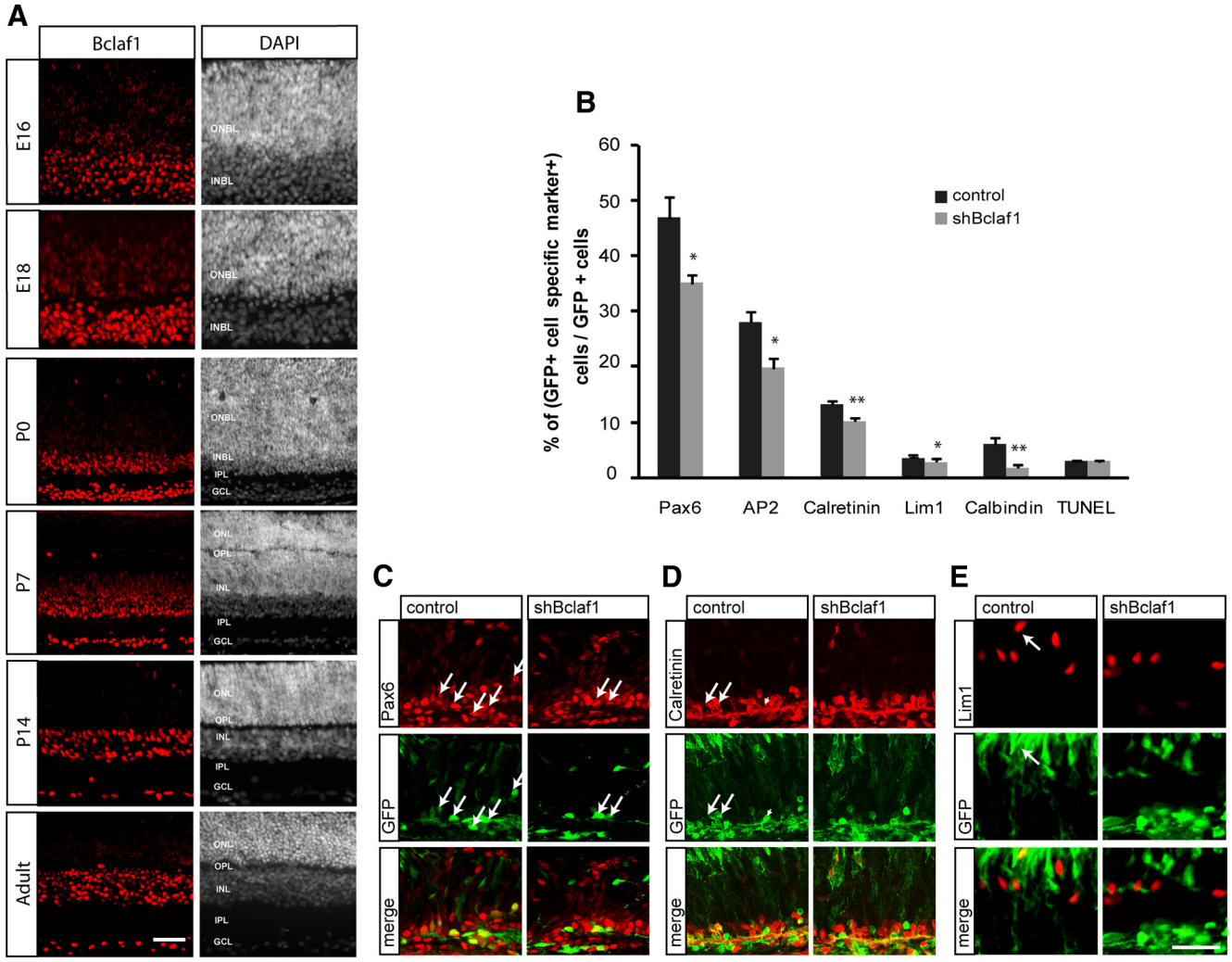

Figure 6. Bclaf1 silencing in early rat RPCs reproduces the retinal phenotype of Bclaf1-deficient mice. ***A***, Rat retinal sections from the indicated developmental stages were immunolabeled with a Bclaf1 rabbit-polyclonal antibody (red) and weakly counterstained with nuclear DAPI (gray). Bclaf1 expression is restricted to the INBL and both the INL and GCL at different developmental stages. ***B–E***, Retinal explants from E16 rats were electroporated with either pU6-shBclaf1-eGFP or pU6shLuciferase-eGFP (control) vectors. After 5 DIV, dissociated cells (***B***) or frozen sections (***C–E***) from retinal explants were double-immunostained with an anti-GFP antibody and antibodies against the indicated cell type. Silencing *Bclaf1* led to a decrease in positive cells for Pax6, AP2, calretinin, Lim1, and calbindin among GFP+ cells (***B***). No differences in cell death were observed after silencing *Bclaf1* compared with control (***B***). Sections stained for GFP and either Pax6 (***C***), calretinin (***D***), or Lim1 (***E***) showed a decrease in double-labeled cells in shBclaf1-electroporated explants. Arrows indicate colabeled cells. Values represent the mean ± SEM (*$p < 0.05$, **$p < 0.01$) from at least three separate retina counts. Scale bar, 50 μm.

plants (Fig. 7*D*,*E*). These results indicate that apoptosis of photoreceptor precursors or differentiating rods contribute to the decreased number of rods after Bclaf1 overexpression in late RPCs.

Molecular mechanisms underlying Bclaf1 effects

To further understand the molecular mechanisms underlying Bclaf1-mediated changes in retinal differentiation, we constructed two different mutants of Bclaf1: Bclaf1-DC210, a truncated form of Bclaf1 that is unable to interact with Bcl-2 proteins (Kasof et al., 1999), and Bclaf1-DN384 which lacks the "SR rich-bZip domain" but is able to bind Bcl-2 proteins and Emerin (Kasof et al., 1999; Mansharamani and Wilson, 2005; Fig. 8*A*,*B*). After fibroblast transfection, Western blot analysis with specific polyclonal antibodies against the C-terminal part or N-terminal part of Bclaf1 confirmed the production of the two mutant forms DC210 and DN384 at the predicted sizes of 25 and 54 kDa respectively (Fig. 8*B*). Immunofluorescence experiments revealed that the DN384 mutant is located exclusively in the cytoplasm in contrast to the full-length form of Bclaf1 and the DC210 mutant which both display nuclear localization (Fig. 8*C*). Electroporation of these mutants in P0 retinal explants revealed that only the overexpression of Bclaf1-DC210 led to the same effects as those observed after the overexpression of the full-length form of Bclaf1, i.e., an increase in the fraction of Pax6-positive cells and a decrease in the fraction of rhodopsin-positive cells (Fig. 8*D*). These results indicate that the SR rich domain of Bclaf1 is required for its effects on retinal differentiation, independently of its interaction with endogenous Bcl-2-related proteins.

Bclaf1 expression pattern during development showed that this factor is preferentially localized in the nucleus of Pax6-positive cells (Figs. 2*B*,*E*, 3). Because leucine-zipper transcription factors such as MafA have been shown to modulate Pax6 transcriptional activity through their bZip domains (Kataoka et al., 2001; Planque et al., 2001), we tested the effect of an enhancement of Pax6 transcriptional activity by Bclaf1 which carries a bZip domain. Cotransfection of the Pax6-dependent glucagon promoter (Planque et al., 2001) with vectors expressing Pax6 and

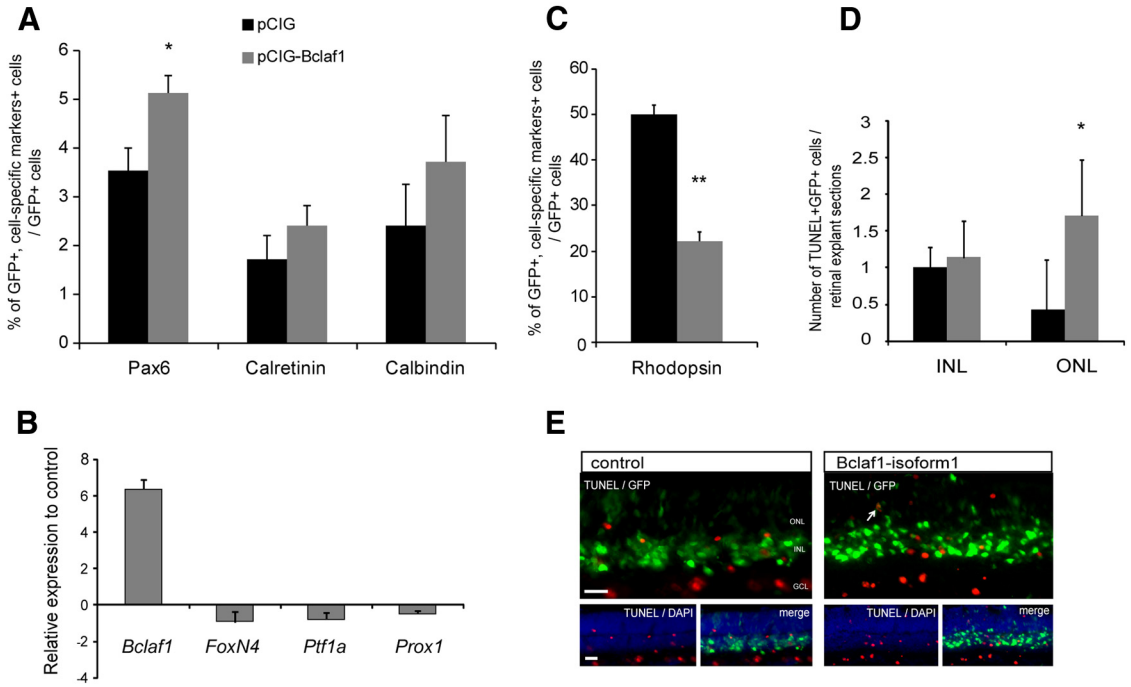

Figure 7. Ectopic expression of Bclaf1 in postnatal retinal explants is not sufficient to bias the cell fate of late progenitors and induces the cell death of differentiating rod photoreceptors. Retinal explants from P0 pups were electroporated with either pCIG-Bclaf1-eGFP or pCIG-eGFP (control) vectors. ***A***, After 7 DIV, dissociated cells from retinal explants were coimmunostained for GFP with Pax6, Calretinin or Calbindin. The graph shows the ratio of specific marker+ cells from the GFP+ cell population. Forced expression of Bclaf1 induced an increase by 45% of Pax6+ cell ratio within GFP+ cell population, compared with control. The ratio of calretinin+ or calbindin+ cells displays no significant difference between the two experimental groups. ***B***, q-PCR on mRNA extracts from FACS sorted GFP-positive cells 36 h after electroporation with pCIG-Bclaf1-eGFP or pCIG-eGFP. *Bclaf1* overexpression is confirmed by the sixfold increase of its relative expression compared with control conditions. By contrast, no significant modification of expression was found for transcription factors required for AC or HC specification such *FoxN4*, *Ptf1*, and *Prox1*. ***C***, Forced expression of Bclaf1 induced a 55.7% decrease of rhodopsin+/GFP+ cell ratio in P0 + 7 DIV retinal explants compared with control. ***D***, ***E***, After 7 DIV, cells undergoing apoptosis were TUNEL-labeled in retinal sections (***E***). Quantitative analysis of GFP+ apoptotic cells in the INL and ONL per section (***D***) showed a significant increase in TUNEL+ cells in pCIG-Bclaf1-eGFP electroporated explants compared with control explants. Values (***A–D***) represent the mean ± SEM (*$p < 0.05$, **$p < 0.01$) from at least three separate retina counts. Scale bars, 50 μm.

Bclaf1 resulted in a threefold increase of promoter activity compared with the level of expression obtained with Pax6 alone (Fig. 8*E*), whereas Bclaf1 alone did not activate the glucagon promoter. The Bclaf1-DC210 mutant form transactivated the glucagon promoter to a similar extent as the full-length Bclaf1, whereas the Bclaf1-DN384 mutant form lost its transactivation property (Fig. 8*E*). Together, these findings indicate that Bclaf1 is able to enhance Pax6 transcriptional activity via its "SR rich–bZip domain." To support this potential role in the retinal context, we evaluated the expression level of three different Pax6 target genes (Marquardt et al., 2001; Shaham et al., 2012) in *Bclaf1*-deficient retina. q-PCR analysis on mRNA extracts from E16.5 retina revealed no significant change in the expression of *Atoh7* but a reduced expression of *Ascl1a* and *Ngn2* by 36% and 38%, respectively, in Bclaf1 $^{-/-}$ mice compared with WT littermates (Fig. 8*F*).

Discussion

Bclaf1 contributes to the differentiation of RGCs, ACs, and HCs

In the present study, we report that the transcription factor Bclaf1 is expressed in Pax6-positive early-born retinal cells and contributes to the differentiation process of RGCs, ACs, and HCs, independently of interactions with anti-apoptotic members of the Bcl-2 family. Analysis of the retinal phenotype of embryonic *Bclaf1*-deficient mice demonstrated a delay in the generation of RGCs, a defective generation of ACs and HCs, and a slightly higher density of cone photoreceptors. Silencing endogenous Bclaf1 expression by electroporation of a shRNA in embryonic retina confirmed that Bclaf1 plays a positive role during AC and HC generation. By contrast, Bclaf1 alone is unable to respecify late RPCs into an AC or HC lineage.

Because Bclaf1 expression begins at E14.5 and is restricted to postmitotic cells, it is unlikely that Bclaf1 could be involved in the fate commitment and initial generation of RGCs, whose specification is initiated earlier at ~E11 in mice (Young, 1985; Yang et al., 2003; Bassett and Wallace, 2012). However, Bclaf1 could potentially contribute to the RGC diversity programming like *Brn3* genes (Badea et al., 2009) or to the terminal differentiation like *Ils1* (Pan et al., 2008), or more probably cooperate with these last genes to ensure proper differentiation of RGCs, as described for early B-cell factors (Jin et al., 2010).The generation of RGCs was only delayed in absence of Bclaf1, because the density of RGCs at E18.5 is comparable in WT and *Bclaf1* $^{-/-}$ retina, suggesting that, although dispensable, Bclaf1 contributes to the timing of the generation of the RGCs. The absence of Bclaf1 could be compensated by other factors, as previously demonstrated for transcription factors Sox11 and Sox4. Indeed, the generation of RGCs is delayed in *Sox11*-deficient mice but compensated for after birth possibly because of the redundant activity of Sox4 (Usui et al., 2013).

Bclaf1 may play a more crucial role in the differentiation and maintenance of ACs and HCs. Indeed, a reduction of 15 and 30% in the numbers of ACs and HCs, respectively, was observed in the retinas of embryonic *Bclaf1* $^{-/-}$ mice and no full compensation was present as far as we could measure. ACs and HCs are generated slightly later than RGCs (Livesey and Cepko, 2001) and be-

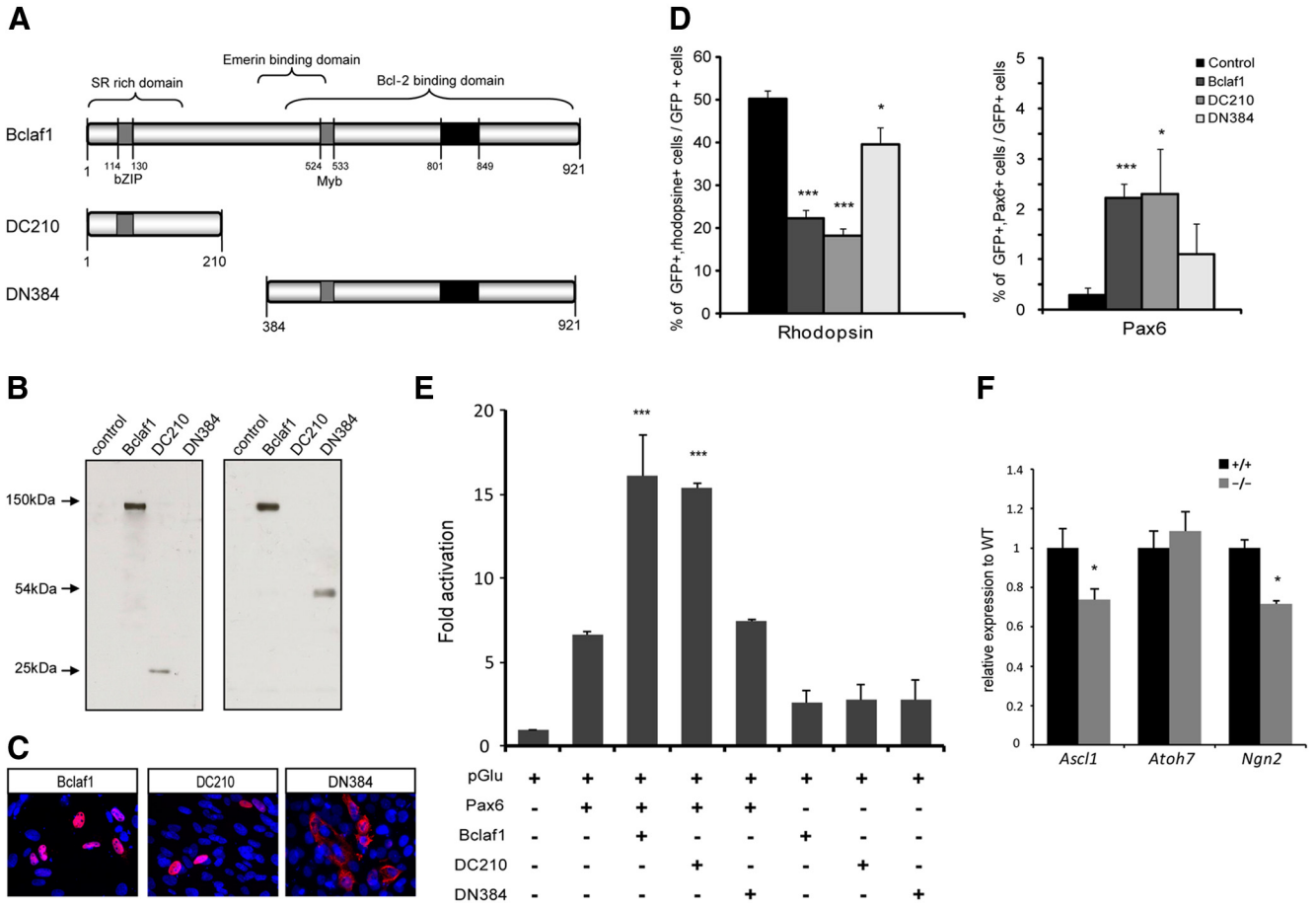

Figure 8. Molecular mechanisms involved in Bclaf1 effects. ***A***, Schematic structure of Bclaf1 mutants. The black box corresponds to the sequence that is lacking in the short isoform. The gray boxes represent the putative bZip and Myb DNA binding domains. ***B***, Expression of the two mutants of Bclaf1, cloned into pCIG-eGFP vector and transfected in DF1 cells. Western-blotting analysis confirmed the production of the two mutant forms DC210 and DN384 at the predicted sizes of 25 and 54 kDa, respectively. Polyclonal and monoclonal antibodies recognized epitopes corresponding to region from residues 150–200 (full form and DC210; left) and 318–439 (full form and DN384; right) respectively. ***C***, Analysis of subcellular localization of the two Bclaf1 mutants in DF1 cells by immunofluorescence. Note that the DN384 mutant is located exclusively in the cytoplasm in contrast to the full-length form of Bclaf1 and the DC210 mutant, which both display nuclear localization. ***D***, Retinal explants from P0 pups were electroporated with either pCIG-Bclaf1-eGFP, pCIG-DC210-eGFP, pCIG-DN384-eGFP or pCIG-eGFP (control) vectors. After 7 DIV, dissociated cells from retinal explants were double-immunostained with an anti-GFP antibody and antibodies against Pax6 or rhodopsin. Only overexpression of DC210 mutant leads to the same effects that full-length form of Bclaf1. ***E***, BHK21 cells were transiently transfected with a reporting vector driving expression of CAT under the control of the glucagon promoter (which is Pax6-dependent), the Pax6-expressing vector, and one of the vectors expressing the distinct mutants of Bclaf1. Bclaf1 alone is unable to transactivate the glucagon promoter but a synergistic effect on the transactivation of the glucagon promoter is observed between Pax6 and Bclaf1 when they are coexpressed, except in the case of the DN384 mutant. The results expressed as mean ± SEM from at least three different experiments were normalized to β-galactosidase activity derived from a cotransfected CMV-LacZ expression plasmid. ***F***, q-PCR on mRNA extracts from E16.5 retina showed that *Ascl1a* and *Ngn2* relative expression was reduced in *Bclaf1*$^{-/-}$ compared with WT embryos. No modification of expression was observed for the *Atoh7* relative expression. Data are expressed as mean ± SEM from three different experiments (*$p < 0.05$, ***$p < 0.001$).

cause in rodents, RPCs switch from early to late identity around birth, we can postulate that thereafter that they will no longer be able to generate enough ACs and HCs to counterbalance the late embryonic deficit in AC and HC generation. Forced expression of Bclaf1 in late RPCs is not sufficient to confer competence to generate early-born neurons like ACs and HCs, presumably because Bclaf1 is not able to induce the expression of genes required for AC and HC production (Dyer et al., 2003; Li et al., 2004; Fujitani et al., 2006), as we demonstrated in the case of the transcription factors *FoxN4*, *Ptf1*, and *Prox1*. Because Bclaf1 is expressed by virtually all ACs, it seems unlikely that Bclaf1 contributes to the specification or the differentiation of a particular subtype of ACs in contrast to others factors such as Bhlb5 or Nr4a2, which contribute to the specification of GABAergic amacrine cells (Feng et al., 2006; Jiang and Xiang, 2009). The homeobox gene *Barhl2,* which is involved in the specification of glycinergic ACs, is expressed like Bclaf1 in postmitotic differentiating RGCs, ACs, and HCs (Mo et al., 2004). However, in contrast to Bclaf1, forced expression of Barhl2 in late RPCs is able to promote the formation of glycinergic ACs at the expense of bipolar and Müller cells (Mo et al., 2004). Nonetheless, forced Bclaf1 expression in postnatal retinal explants shifted the proportions of neuronal cell types generated with an increase in Pax6-positive cells and a reduction in rod photoreceptors. This may be a result of the forced re-expression of Pax6 in late RPCs, which normally give rise to rods, bipolar, and Müller cells, thus hijacking their original cell fate. However, the incapacity of Bclaf1 to readily confer competence to generate early-born neurons is inconsistent with this hypothesis. Alternatively, the increase in the Pax6-positive cell ratio could result from a specific cell death among the non-Pax6-expressing cells. The increase of apoptotic cell number specifically in the ONL after forced expression of Bclaf1 is in agreement with this hypothesis. Selective cell death of Bclaf1-expressing late RPCs and/or rod precursors could potentially ex-

plain the decrease in the proportion of rhodopsin-positive cells and the resulting increase in the proportion of Pax6-positive cells. In addition, it suggests that the survival of late-born cells is compromised by the ectopic expression of a factor specifically expressed in early-born cells.

Among the early-born cells, cone photoreceptors are unique in their lack of Bclaf1 expression. A higher density of differentiating cone photoreceptors (RXRγ- and cone arrestin-positive cells) is present in *Bclaf1*-deficient retinas thus suggesting that the absence of Bclaf1 may favor the differentiation into the cone lineage. On the other hand, Bclaf1 absence does not influence the generation of rod photoreceptors (Otx2-positives or Crx-positives) from late RPCs and therefore, it appears that the higher density of cone photoreceptors in *Bclaf1*$^{-/-}$ retinas is specific to this cell type. Cone photoreceptors are generated earlier than rod photoreceptors and more or less in the same time window than ACs and HCs (Bassett and Wallace, 2012). It was suggested that the cone lineage could be the default pathway for photoreceptor differentiation (Swaroop et al., 2010). Some *Bclaf1*-deficient early-born cells may therefore switch from an AC/HC fate to a cone photoreceptor fate which may represent the only other fate alternative for cells that are being generated at that time. It is, unlikely that Bclaf1 participates directly in the specification and differentiation of cone photoreceptors, such as previously reported for specific nuclear receptors (Swaroop et al., 2010) and the transcription factor from the Spalt family, Sall3 (de Melo et al., 2011). Our experimental data implicates Bclaf1 as a factor that is most likely helping early precursors to differentiate rather than as an instructive factor, such as Ptf1a (Fujitani et al., 2006; Lelièvre et al., 2011).

Mechanisms of Bclaf1-mediated regulation of retinal development

Domain deletion analysis showed that truncation of the RS domain of Bclaf1 (Bclaf1-DN384) abolished its effect on RPC differentiation, whereas a Bclaf1 mutant with the C-terminal deletion (Bclaf1-DC210) retained most of its activity. Thus, the domain necessary for interaction with Bcl-2 is not required for Bclaf1 to exert its effects. This suggests that Bclaf1 plays a role independent of apoptosis during retinal development as previously reported for Bclaf1 in development (McPherson et al., 2009; Sarras et al., 2010). Conversely, the N-terminal domain, which is sufficient to repress transcription (Kasof et al., 1999) and which contains both the RS and bZip domains, was essential for Bclaf1 function in the retina. RS-containing proteins are typically linked with pre mRNA biogenesis and processing events. Various studies have already identified Bclaf1 as an actor in processes governing RNA metabolism, such mRNA splicing and processing (Merz et al., 2007; Bracken et al., 2008; Sarras et al., 2010). It is tempting to speculate whether the role of Bclaf1 in regulating mRNA processing events could explain its role in retinal development. Bclaf1 might also participate in the control of alternative splicing of bHLH transcription factors and/or the regulation of mRNA translation of retinal homeogenes, two processes that have been involved in retinal specification and differentiation (Decembrini et al., 2006).

Another mechanism whereby Bclaf1 could mediate its effect is through its ability to enhance Pax6 transcriptional activity. We showed that Bclaf1 acts in synergy with Pax6 to activate the glucagon promoter. The presence of the bZip domain was necessary to mediate this effect in agreement with previous studies reporting that the domain spanning the basic region and the leucine zipper structure of other bZip factors is required for association with Hox proteins (Kataoka et al., 2001). In the developing retina, Bclaf1 and Pax6 expression patterns are very similar, suggesting that a functional synergy between Bclaf1 and Pax6 may occur in postmitotic precursors to facilitate their differentiation into ACs, HCs, or RGCs. The reduced expression of the two Pax6 target genes, *Ascl1a* and *Ngn2*, in E16.5 Bclaf1-deficient retina supports this hypothesis. Although the physical interaction between these two transcription factors remains to be established, functional synergy between Pax6 and Bclaf1 might also participate in the prevention of photoreceptor differentiation, because Pax6 has been identified as a potential repressor of Crx expression (Oron-Karni et al., 2008). Furthermore, if Bclaf1 functions are dependent on Pax6, the absence of Pax6 expression in late RPCs could explain why Bclaf1 is unable to bias their commitment.

In conclusion, our results have shown that Bclaf1 contributes to the differentiation of early precursors into RGCs, ACs, and HCs instead of cone photoreceptors. Moreover, our data indicates that Bclaf1 participates in the differentiation process of RGCs, ACs, and HCs as a transcription factor, rather than via its interaction with Bcl-2-related proteins, and most probably by potentiating the activity of Pax6.

References

Badea TC, Cahill H, Ecker J, Hattar S, Nathans J (2009) Distinct roles of transcription factors brn3a and brn3b in controlling the development, morphology, and function of retinal ganglion cells. Neuron 61:852–864. CrossRef Medline

Bassett EA, Wallace VA (2012) Cell fate determination in the vertebrate retina. Trends Neurosci 35:565–573. CrossRef Medline

Boy S, Souopgui J, Amato MA, Wegnez M, Pieler T, Perron M (2004) XSEB4R, a novel RNA-binding protein involved in retinal cell differentiation downstream of bHLH proneural genes. Development 131:851–862. CrossRef Medline

Bracken CP, Wall SJ, Barré B, Panov KI, Ajuh PM, Perkins ND (2008) Regulation of cyclin D1 RNA stability by SNIP1. Cancer Res 68:7621–7628. CrossRef Medline

Cayouette M, Poggi L, Harris WA (2006) Lineage in the vertebrate retina. Trends Neurosci 29:563–570. CrossRef Medline

Decembrini S, Andreazzoli M, Vignali R, Barsacchi G, Cremisi F (2006) Timing the generation of distinct retinal cells by homeobox proteins. PLoS Biol 4:e272. CrossRef Medline

Decembrini S, Bressan D, Vignali R, Pitto L, Mariotti S, Rainaldi G, Wang X, Evangelista M, Barsacchi G, Cremisi F (2009) MicroRNAs couple cell fate and developmental timing in retina. Proc Natl Acad Sci U S A 106:21179–21184. CrossRef Medline

de Melo J, Peng GH, Chen S, Blackshaw S (2011) The Spalt family transcription factor Sall3 regulates the development of cone photoreceptors and retinal horizontal interneurons. Development 138:2325–2336. CrossRef Medline

Dyer MA, Livesey FJ, Cepko CL, Oliver G (2003) Prox1 function controls progenitor cell proliferation and horizontal cell genesis in the mammalian retina. Nat Genet 34:53–58. CrossRef Medline

Feng L, Xie X, Joshi PS, Yang Z, Shibasaki K, Chow RL, Gan L (2006) Requirement for Bhlhb5 in the specification of amacrine and cone bipolar subtypes in mouse retina. Development 133:4815–4825. CrossRef Medline

Fujitani Y, Fujitani S, Luo H, Qiu F, Burlison J, Long Q, Kawaguchi Y, Edlund H, MacDonald RJ, Furukawa T, Fujikado T, Magnuson MA, Xiang M, Wright CV (2006) Ptf1a determines horizontal and amacrine cell fates during mouse retinal development. Development 133:4439–4450. CrossRef Medline

Furukawa T, Morrow EM, Cepko CL (1997) Crx, a novel otx-like homeobox gene, shows photoreceptor-specific expression and regulates photoreceptor differentiation. Cell 91:531–541. CrossRef Medline

Georgi SA, Reh TA (2010) Dicer is required for the transition from early to late progenitor state in the developing mouse retina. J Neurosci 30:4048–4061. CrossRef Medline

Haraguchi T, Holaska JM, Yamane M, Koujin T, Hashiguchi N, Mori C, Wilson KL, Hiraoka Y (2004) Emerin binding to Btf, a death-promoting

transcriptional repressor, is disrupted by a missense mutation that causes Emery-Dreifuss muscular dystrophy. Eur J Biochem 271:1035–1045. CrossRef Medline

Hatakeyama J, Tomita K, Inoue T, Kageyama R (2001) Roles of homeobox and bHLH genes in specification of a retinal cell type. Development 128: 1313–1322. Medline

Hwang W, Hackler L Jr, Wu G, Ji H, Zack DJ, Qian J (2012) Dynamics of regulatory networks in the developing mouse retina. PLoS One 7:e46521. CrossRef Medline

Jia L, Oh ECT, Ng L, Srinivas M, Brooks M, Swaroop A, Forrest D (2009) Retinoid-related orphan nuclear receptor RORbeta is an early-acting factor in rod photoreceptor development. Proc Natl Acad Sci U S A 106: 17534–17539. CrossRef Medline

Jiang H, Xiang M (2009) Subtype specification of GABAergic amacrine cells by the orphan nuclear receptor Nr4a2/Nurr1. J Neurosci 29:10449–10459. CrossRef Medline

Jin K, Jiang H, Mo Z, Xiang M (2010) Early B-cell factors are required for specifying multiple retinal cell types and subtypes from postmitotic precursors. J Neurosci 30:11902–11916. CrossRef Medline

Kasof GM, Goyal L, White E (1999) Btf, a novel death-promoting transcriptional repressor that interacts with Bcl-2-related proteins. Mol Cell Biol 19:4390–4404. Medline

Kataoka K, Yoshitomo-Nakagawa K, Shioda S, Nishizawa M (2001) A set of Hox proteins interact with the Maf oncoprotein to inhibit its DNA binding, transactivation, and transforming activities. J Biol Chem 276:819–826. Medline

Lamy L, Ngo VN, Emre NC, Shaffer AL 3rd, Yang Y, Tian E, Nair V, Kruhlak MJ, Zingone A, Landgren O, Staudt LM (2013) Control of autophagic cell death by caspase-10 in multiple myeloma. Cancer Cell 23:435–449. CrossRef Medline

Lelièvre EC, Lek M, Boije H, Houille-Vernes L, Brajeul V, Slembrouck A, Roger JE, Sahel JA, Matter JM, Sennlaub F, Hallböök F, Goureau O, Guillonneau X (2011) Ptf1a/Rbpj complex inhibits ganglion cell fate and drives the specification of all horizontal cell subtypes in the chick retina. Dev Biol 358:296–308. CrossRef Medline

Lelièvre EC, Benayoun BA, Mahieu L, Roger JE, Sahel JA, Sennlaub F, Veitia RA, Goureau O, Guillonneau X (2012) A regulatory domain is required for Foxn4 activity during retinogenesis. J Mol Neurosci 46:315–323. CrossRef Medline

Li S, Mo Z, Yang X, Price SM, Shen MM, Xiang M (2004) Foxn4 controls the genesis of amacrine and horizontal cells by retinal progenitors. Neuron 43:795–807. CrossRef Medline

Liu H, Lu ZG, Miki Y, Yoshida K (2007) Protein kinase Cδ induces transcription of the TP53 tumor suppressor gene by controlling death-promoting factor Btf in the apoptotic response to DNA damage. Mol Cell Biol 27:8480–8491. CrossRef Medline

Livesey FJ, Cepko CL (2001) Vertebrate neural cell-fate determination: lessons from the retina. Nat Rev Neurosci 2:109–118. CrossRef Medline

Maiorano NA, Hindges R (2012) Non-coding RNAs in retinal development. Int J Mol Sci 13:558–578. CrossRef Medline

Mansharamani M, Wilson KL (2005) Direct binding of nuclear membrane protein MAN1 to emerin in vitro and two modes of binding to barrier-to-autointegration factor. J Biol Chem 280:13863–13870. CrossRef Medline

Marquardt T, Ashery-Padan R, Andrejewski N, Scardigli R, Guillemot F, Gruss P (2001) Pax6 is required for the multipotent state of retinal progenitors cells. Cell 105:43–55. CrossRef Medline

Matter-Sadzinski L, Puzianowska-Kuznicka M, Hernandez J, Ballivet M, Matter J-M (2005) A bHLH transcriptional network regulating the specification of retinal ganglion cells. Development 132:3907–3921. CrossRef Medline

Mears AJ, Kondo M, Swain PK, Takada Y, Bush RA, Saunders TL, Sieving PA, Swaroop A (2001) Nrl is required for rod photoreceptor development. Nat Genet 29:447–452. Medline

McPherson JP, Sarras H, Lemmers B, Tamblyn L, Migon E, Matysiak-Zablocki E, Hakem A, Azami SA, Cardoso R, Fish J, Sanchez O, Post M, Hakem R (2009) Essential role for Bclaf1 in lung development and immune system function. Cell Death Differ 16:331–339. CrossRef Medline

Merz C, Urlaub H, Will CL, Lührmann R (2007) Protein composition of human mRNPs spliced in vitro and differential requirements for mRNP protein recruitment. RNA 13:116–128. CrossRef Medline

Mo Z, Li S, Yang X, Xiang M (2004) Role of the Barhl2 homeobox gene in the specification of glycinergic amacrine cells. Development 131:1607–1618. CrossRef Medline

Oron-Karni V, Farhy C, Elgart M, Marquardt T, Remizova L, Yaron O, Xie Q, Cvekl A, Ashery-Padan R (2008) Dual requirement for Pax6 in retinal progenitor cells. Development 135:4037–4047. CrossRef Medline

Pan L, Deng M, Xie X, Gan L (2008) ISL1 and BRN3B co-regulate the differentiation of murine retinal ganglion cells. Development 135:1981–1990. CrossRef Medline

Planque N, Leconte L, Coquelle FM, Benkhelifa S, Martin P, Felder-Schmittbuhl MP, Saule S (2001) Interaction of Maf transcription factors with Pax-6 results in synergistic activation of the glucagon promoter. J Biol Chem 276:35751–35760. CrossRef Medline

Rapaport DH, Wong LL, Wood ED, Yasumura D, LaVail MM (2004) Timing and topography of cell genesis in the rat retina. J Comp Neurol 474: 304–324. CrossRef Medline

Rénert AF, Leprince P, Dieu M, Renaut J, Raes M, Bours V, Chapelle JP, Piette J, Merville MP, Fillet M (2009) The proapoptotic C16-ceramide-dependent pathway requires the death-promoting factor Btf in colon adenocarcinoma cells. J Proteome Res 8:4810–4822. CrossRef Medline

Roger J, Brajeul V, Thomasseau S, Hienola A, Sahel JA, Guillonneau X, Goureau O (2006) Involvement of Pleiotrophin in CNTF-mediated differentiation of the late retinal progenitor cells. Dev Biol 298:527–539. CrossRef Medline

Roger J, Goureau O, Sahel JA, Guillonneau X (2007) Use of suppression subtractive hybridization to identify genes regulated by ciliary neurotrophic factor in postnatal retinal explants. Mol Vis 13:206–219. Medline

Sarras H, Alizadeh Azami S, McPherson JP (2010) In search of a function for BCLAF1. ScientificWorldJournal 10:1450–1461. CrossRef Medline

Shaham O, Menuchin Y, Farhy C, Ashery-Padan R (2012) Pax6: a multi-level regulator of ocular development. Prog Retin Eye Res 31:351–376. CrossRef Medline

Swaroop A, Kim D, Forrest D (2010) Transcriptional regulation of photoreceptor development and homeostasis in the mammalian retina. Nat Rev Neurosci 11:563–576. CrossRef Medline

Usui A, Mochizuki Y, Iida A, Miyauchi E, Satoh S, Sock E, Nakauchi H, Aburatani H, Murakami A, Wegner M, Watanabe S (2013) The early retinal progenitor-expressed gene Sox11 regulates the timing of the differentiation of retinal cells. Development 140:740–750. CrossRef Medline

Yang Z, Ding K, Pan L, Deng M, Gan L (2003) Math5 determines the competence state of retinal ganglion cell progenitors. Dev Biol 264:240–254. CrossRef Medline

Young RW (1985) Cell differentiation in the retina of the mouse. Anat Rec 212:199–205. CrossRef Medline